

## Laser Thomson Scattering and Optical Emission Studies of PDP

**Hassaballa, Safwat**

Department of Applied Science for Electronics and Materials, Graduate School of Engineering  
Science, Kyushu University

**Tomita, Kentaro**

Department of Applied Science for Electronics and Materials, Graduate School of Engineering  
Science, Kyushu University

**Kim, Young Kee**

Department of Applied Science for Electronics and Materials, Graduate School of Engineering  
Science, Kyushu University

**Uchino, Kiichiro**

Department of Applied Science for Electronics and Materials, Graduate School of Engineering  
Science, Kyushu University

<https://doi.org/10.15017/16736>

---

出版情報 : 九州大学大学院総合理工学報告. 26 (3), pp.327-332, 2004-12. 九州大学大学院総合理工学  
府

バージョン :

権利関係 :

# Laser Thomson Scattering and Optical Emission Studies of PDP Micro-Discharge Plasmas

Safwat HASSABALLA<sup>\*1,†</sup>, Kentaro TOMITA<sup>\*1</sup>, Young Kee KIM<sup>\*1</sup>,  
and Kiichiro UCHINO<sup>\*1</sup>

<sup>†</sup>E-mail of corresponding author: uchino@ence.kyushu-u.ac.jp

(Received October 29, 2004)

Properties of a plasma display panel (PDP) like discharge were examined by emission and laser Thomson scattering (LTS) measurements. Emission measurements were performed using an intensified CCD camera. By varying several external parameters such as amplitude of the input voltage, gas composition and pressure, the influence of these parameters on the discharge behavior was studied. Results of emission measurements showed that they were in good agreement with similar emission measurements on real PDP cells. LTS measurements were performed for the discharge at a pressure of 100 Torr. The results yielded precise profiles of electron density and electron temperature of the striated PDP-like plasma for the first time.

**Key words:** *Plasma display panel, laser Thomson scattering, optical emission*

## 1. Introduction

A plasma display panel (PDPs) is one of large-area flat panel displays which are now widely spreading for business and private use. PDP has some superior features such as excellent image quality and being suitable for the mass production of the large size panel even more than 100 inches. The major drawback of the PDP is the low luminous efficiency, which is still less than 2 lm/Watt and is much less than that of conventional CRTs (about 5 lm/Watt). Therefore, improvement of the luminous efficiency will lead to distinctive reduction in power consumption and then to wider use of PDP.<sup>1,2)</sup>

PDPs are normally operated in Ne/Xe gas mixtures at a pressure of 500 Torr, using a discharge gap of about 100  $\mu\text{m}$ . Due to the high pressure and the small discharge gap, it is considered that the cathode fall dominates most of the discharge area, causing a decrease in the discharge efficiency. To improve the PDP luminous efficiency, it is important to improve the efficiency of the PDP micro-discharges in generating UV photons.

The PDP discharges are featured by small dimensions and short duration of 100 ns. In order to diagnose the PDP micro-discharges,

high spatio-temporal resolution is required. For the purpose, a laser Thomson scattering (LTS) system has been developed to directly measure electron density  $n_e$  and electron temperature  $T_e$  profiles in PDP micro-discharge plasmas.<sup>3, 4, 5)</sup> Previously, LTS measurements were performed at a height of 100  $\mu\text{m}$  above the electrode surface to measure spatio-temporal distributions of  $n_e$  and  $T_e$  along the electrode surface.<sup>3)</sup> Recently, the spatial resolution has been improved to about 50  $\mu\text{m}$ , which allowed approaching to the point as close as 60  $\mu\text{m}$  from the electrode surface. Measurements were done in horizontal and vertical directions above the electrode surface, to determine two-dimensional distribution of  $n_e$  and  $T_e$  at different discharge times and pressures.<sup>4,5)</sup>

The drawback of the LTS method is that it is elaborate and time consuming to perform measurements at many space and time points. Therefore, it is desirable to roughly observe the discharge structure using some means before performing LTS measurements. Especially, it is known that striation structures of optical emission images universally appear in ac-PDP discharges.<sup>2)</sup> In order to record such emission images, an image intensified CCD (ICCD) camera is the most powerful tool.

In this study, we extensively examined spatial and temporal changes of emission images of PDP-like discharges under various

<sup>\*1</sup> Department of Applied Science for Electronics and Materials, Interdisciplinary Graduate School of Engineering Sciences, Kyushu University

conditions using the ICCD camera. Then, detailed measurements of  $n_e$  and  $T_e$  distributions of the striated PDP-like plasma were performed using the LTS method under one discharge condition, and the results were tried to relate with the corresponding optical emission image.

## 2. Experimental Setup

The electrode configurations and the experimental setup for LTS scattering measurements have been described in detail in Fig.1 shows the experimental setup for the ICCD imaging measurements, which were carried out under similar discharge conditions as in previous LTS studies. The ICCD camera was adjusted to operate in the gate mode, where high temporal resolution measurements were desired. The gate width of the ICCD camera has been adjusted at 20 ns. Emissions from the plasmas were collected using a lens having a focal length of 125 mm. Because of the small dimensions of the PDP discharge, the lens was adjusted to produce a 1:3 magnification. Depending on the emission intensity the signals were accumulated 50 or 100 times to enhance the resolution.

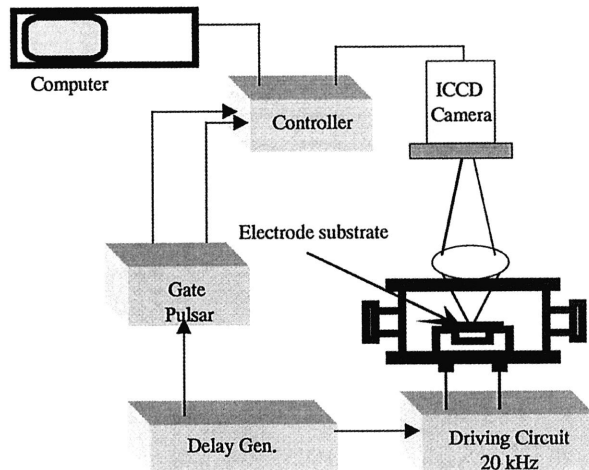


Fig. 1 A schematic diagram of the emission measurements using ICCD Camera.

The behavior of the discharge was studied experimentally under the following conditions:  
1- Gas pressure, 100 Torr – 500 Torr  
2- Gas composition, Ne/Ar (0,10,20%), Ne/Kr (5,10%) and Ne/Xe (5,10%)  
3- Discharge voltage, 220, 240 and 280 Volt  
4- Electrode geometry, electrode gaps of 0.1 and 1 mm were employed to proof the validation of scaling laws. The Electrode length was minimized by two barrier ribs

centered on the gap at  $\pm 1$  mm. Moreover, measurements at different wavelengths using several band pass filters were done in order to analyze the emission distributions along the electrode surface.

## 3. Results and Discussion

### 3.1 Temporal evolution of the discharge

Figure 2 shows the total integrated emission images taken by the ICCD camera for a Ne/Ar (10%) gas admixture at a gas pressure of 200 Torr. The applied voltage was 240 Volt. The length of the discharge was controlled using barrier ribs at a distance of  $\pm 1$  mm from the gap.

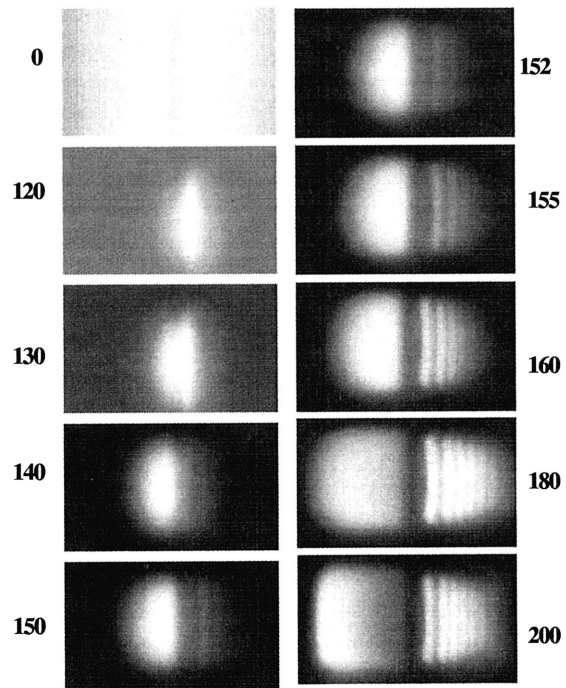


Fig. 2 Emission images taken by the ICCD camera at different times after starting the discharge pulse.

As can be seen from Fig. 2, light emissions first appear above the anode, at about 100 ns, and propagate towards the cathode side, away from the dielectric surface above the coplanar electrodes. At 140 ns the glow is above the cathode surface and starts to spread above the cathode. At 150 ns some light emission appears again above the anode, in a very localized region. While the plasma continues spreading along the cathode, a second localized light-emitting region well separated from the first one, forms above the anode at about 155 ns. These localized regions or striations gradually increase with time, and their position was fixed. The first striation close to the discharge gap is more intense than the

others. The instant of maximum current was reached after 180 ns. Then the current decreased and the ICCD images showed a decrease in the intensity of the light emitted by the plasma. The spreading of the plasma above the anode and the cathode belongs to the progressive charging of the dielectric surfaces.

This temporal evolution of the PDP discharges has been observed in other experiments and simulations, and can be explained in terms of charged particle densities as follows.<sup>6,7)</sup>

After starting the discharge pulse, the electric field is set between the anode and the cathode. This field is almost uniform as long as the charged particle densities are too small to distort it. During this stage the electron density peak is found on the anode side of the discharge.

The distortion of the field induces a fast increase in the electron multiplication. Since electrons are more mobile than ions, they move faster than ions and rapidly reach the anode surface to form the negative surface charge, so there are more ions in space. As long as the electron multiplication is larger than that required for self-sustainment, the plasma region expands towards the cathode side of the discharge.

As the discharge evolves, increased ions slowly drift towards the cathode, which results in a formation of the cathode fall until the decreased overall field cannot maintain the discharge anymore.

### 3.2 Pressure dependence of the discharge evolution

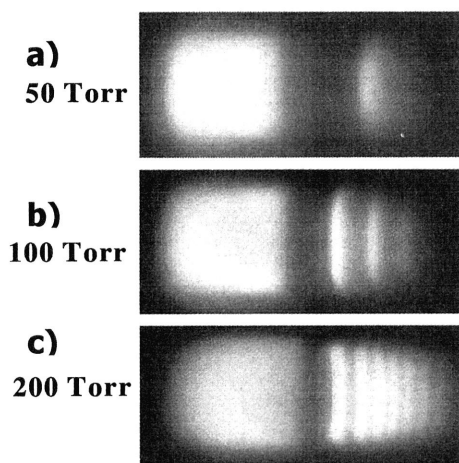


Fig. 3 Emission images taken by the ICCD camera at different pressures at the current peak.

The values of  $pd$  (pressure ( $p$ )  $\times$  discharge gap ( $d$ )) in PDP cells are generally at around the Paschen minimum. If the pressure is increased, the minimum voltage required to sustain the discharge is also increased.

As can be seen from the ICCD images of Ne/Ar (10%) gas at different pressures of 50, 100 and 200 Torr in Fig. 3, the emission intensity increases with pressure. In PDP three body collisions are the dominant reactions responsible for excitations, because they are efficient at higher pressures. It is clear from the figure also that the size of striations (striation width) and the distance between striations decreasing by increasing the pressure. The number of striations also found to be increasing with pressure.

The lagging time (the time from the starting of the voltage pulse to the maximum intensity or the current peak) was shorter for high-pressure discharges. At a constant applied voltage of 240 Volt, the times were found to be 400, 230 and 180 ns for pressures of 50, 100 and 200 Torr, respectively.

### 3.3 Gas composition dependence of the discharge evolution

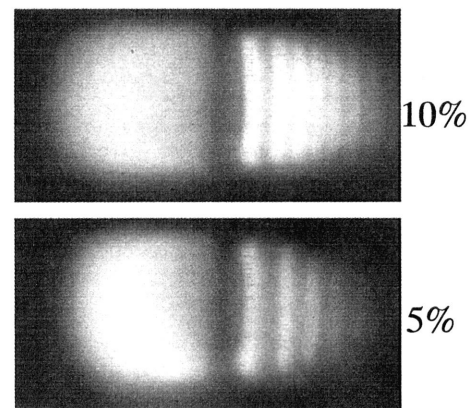


Fig. 4 Emission images taken by the ICCD camera at different Ar percentages.

ICCD camera images of discharges in the Ne/Ar gas at a pressure of 200 Torr are shown in Fig. 4 for different Ar percents (5 and 10%). The emission intensities were increased together with the Ar content. It should be noted that the distance between striations and striation widths increased by decreasing the Ar percentage in the gas mixture. The lagging time was shorter in case of higher Ar content discharges.

Emission profiles of Ne/Kr (5 %) and Ne/Xe (5 %) gas admixtures were also measured. The

fundamental discharge behavior for these gas mixtures was the same as that for the gas mixture Ne/Ar(5 %). Only small discrepancies were found to be attributable to different ionization energies and ion masses which affect the temporal evolution. For example, the discharge develops faster in case of the Ar discharge compared to Kr and Xe gas discharges.

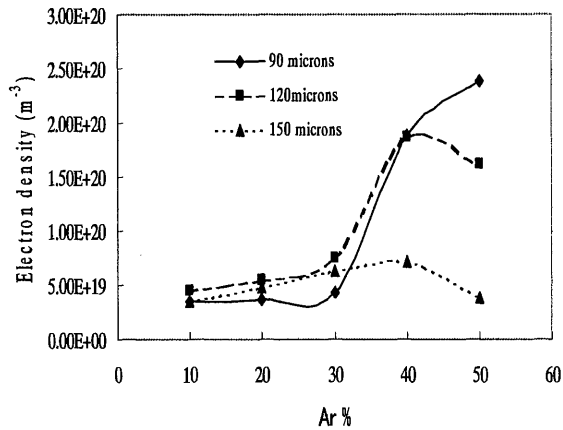


Fig. 5 Variation of the electron density with Ar percentage in the Ne/Ar gas mixture at 200 Torr.

The variation of electron density with Ar percentage in the Ne/Ar gas mixture measured using the LTS method is shown in Fig. 5. Results in Fig. 5 were measured at different heights 90, 120, 150  $\mu\text{m}$  above the discharge gap. As can be seen from the figure, the electron density increases as the Ar percentage increases. The discharge was less spatially extended in case of higher Ar percentages. This decrease in the spatial extension of the discharge is due to the decrease in the diffusion coefficient caused by the increase in the weight density of the discharge gas.

### 3.4 Input voltage dependence of the discharge evolution

Optical emission measurements using the ICCD camera showed that the emission intensities increased together with the increase of the applied voltage. The variation of the current waveforms with the change of the applied voltage is shown in Fig. 6, for the Ne/Ar (10%) admixture at a gas pressure of 100 Torr. Values of the applied voltage amplitude were 180, 200, 220 and 240 Volt.

It can be noticed from the Fig. 6 that, first, the current amplitude increases with the increase of the applied voltage. Second, the

lagging time is inversely proportional to the applied voltage amplitude. In the case of voltage amplitude of 180 Volt, the lagging time was about 350 ns, compared to about 220 ns in the case of 240 Volt. This lagging time can be considered to depend on the number of charged particles remaining from the previous discharge pulse. Since this number of charged particles increase with the applied voltage, then the discharge ignition is slower in the case of lower applied voltage. Actually, electron density measurements using the LTS method for discharges in the gas mixture of Ne/Ar (10%) at a pressure of 200 Torr with applied voltages of 220, 240 and 280 Volt showed that the electron density increase with the increase of the applied voltage.

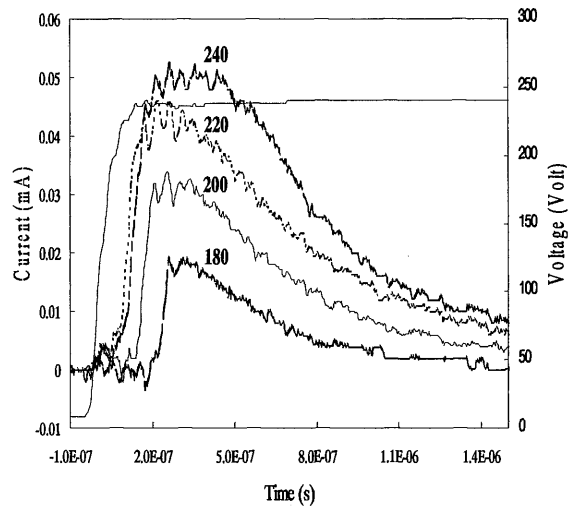


Fig. 6 Variation of the current waveform for different applied voltages.

### 3.5 Visible and infrared emissions

Several band pass filters at different central wavelengths were used to observe distributions of the different emissions from the discharge. All the ICCD images taken at different experimental conditions showed that the visible light emissions were mainly located at the cathode side. This corresponds to the classical negative glow emission, which result from atomic excitations by energetic electrons accelerated in the cathode sheath. These visible emissions are mainly from the excited states of the Ne gas. Infrared (IR) emissions were distributed between both the cathode and anode sides. These infrared emissions are mainly from the excited Ar species. It is well known that the area above anode region is

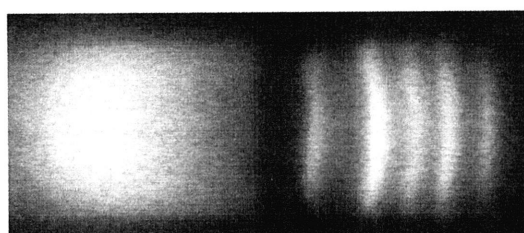
more efficient for Ar IR excitations.

### 3.6 Macro-gap electrode

Real PDPs have a discharge gap of about 100  $\mu\text{m}$  and normally operate at high gas pressures in the range of 400-500 Torr. Since the cell dimensions of the real PDPs are difficult to access experimentally, use of a macro-gap cell can be a good solution to overcome the problem. The macro-gap electrodes are electrodes having a gap size in the range of 1-10 mm. In this case, the pressure will be 10-100 times lower than the real PDP gas pressure. The experimental access of the macro-gap electrodes will be much easier than the real PDP cell electrodes.<sup>9)</sup>

The similarity laws predict that glow discharges having the same ( $pd$ ) have “similar” properties at the same ( $pt$ ) (pressure multiplied by time), if the same voltage is applied to the electrodes. This means that, for example, the properties of a discharge with a 100  $\mu\text{m}$  gap at a pressure of 500 Torr (typical condition of the PDP discharge) can be deduced from the properties of a discharge operating in a 1 mm gap at a pressure of 50 Torr. The recombination rate, which is a function of the gas pressure, determines the validity of these scaling laws.

Two macro-gap electrodes have been fabricated. The electrodes have a 1 mm discharge gap, and the widths of the electrodes were 3 and 5 mm. The gas pressure was set at 20 Torr so that the product  $pd$  became 2 as the case of the 100  $\mu\text{m}$  gap electrode at a pressure of 200 Torr. The applied voltage was 210 V. The optical emission image of a macro-gap discharge at a gas pressure of 20 Torr is shown in Fig. 8. It is clear from the figure that the emission image of the 1 mm gap discharge is similar to that of the 100  $\mu\text{m}$  gap discharge.



cathode anode

Fig. 8 Emission image of the macro-gap discharge at a gas pressure of 20 Torr.

Results of LTS measurements of Ne-Ar (10%) at a pressure of 20 Torr for the macro-gap electrode showed that  $n_e$  and  $T_e$  were  $5.6 \times 10^{18} \text{ m}^{-3}$  and 1.05 eV, respectively. The value of  $n_e$  measured for the 1 mm gap electrode was one order of magnitude less than that for the 100  $\mu\text{m}$  gap electrode. This fact indicates a scaling law that  $n_e$  is proportional to the gas pressure.

### 3.7 $n_e$ and $T_e$ profiles of the striated discharge at 100 Torr

Spatial distributions of  $n_e$  and  $T_e$  have been measured for the discharge produced in Ne/Ar (10%) at a pressure of 200 Torr.<sup>9)</sup> The LTS measurements showed modulations in both  $n_e$  and  $T_e$  profiles. On the other hand, optical emission measurements by the ICCD camera showed modulations in the total emission intensity profiles. It is of interest to compare peak positions of these modulations.

To confirm whether the first peak in the emission profile corresponds to the  $n_e$  peak or the  $T_e$  peak, we performed LTS and optical emission measurements for the discharge at a pressure of 100 Torr gas. In this condition, the distance between the striations is large enough to be resolved by the LTS measurements.

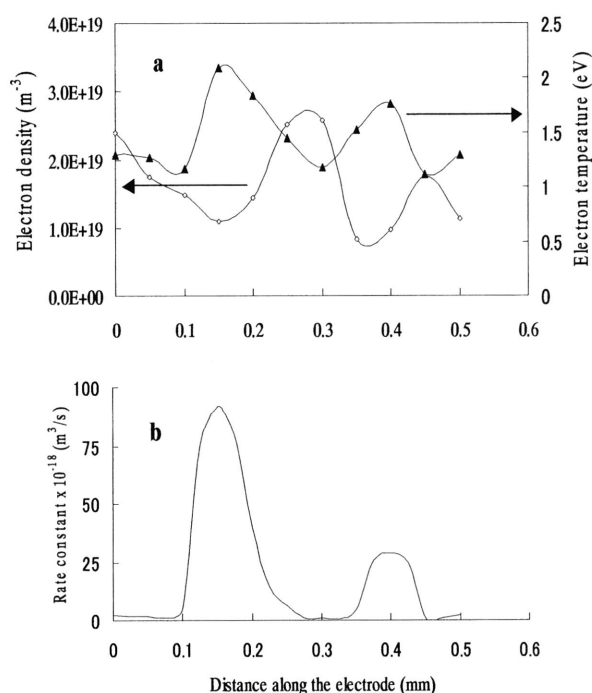


Fig. 9 Measured profiles of  $n_e$  and  $T_e$  for Ne/Ar (10%) at a pressure of 100 Torr (a), and calculated modulations in the rate constant for excitation (b).

Spatial distributions of  $n_e$  and  $T_e$  along the anode surface for Ne/Ar (10%) at a pressure of 100 Torr (Fig. 9) showed a similar trend to the discharge produced in the gas at 200 Torr. Modulations in  $n_e$  and  $T_e$  were clearly observed above the anode side. As can be seen from Fig. 9(a), the distances of the density and temperature peaks are 200-250  $\mu\text{m}$ , compared to a distance of 100-150  $\mu\text{m}$  in the case of the 200 Torr discharge.

A simple comparative study of the variation of the rate coefficients for electron impact excitation has been done. The rate coefficient for an electron impact excitation is obtained by integrating the product of the cross section  $\sigma$  and the electron velocity  $v$  over assumed Maxwellian distribution.

$$\kappa = \langle \sigma(v)v \rangle_v = 4\pi \int_0^{\infty} \sigma(v)v^3 f(v)dv$$

where

$$f(v) = \left( \frac{m_e}{2\pi e T_e} \right)^{3/2} \exp\left(-\frac{m_e v^2}{2e T_e}\right)$$

is the Maxwellian velocity distribution function,  $m_e$  is the electron mass,  $e$  is the electron charge.

The experimentally measured electron temperatures have been used to deduce the values of the excitation rate constant.<sup>10</sup> The result of calculation is shown in Fig. 9(b). As can be seen from the figure, the calculated rate coefficient shows modulation along the anode surface. The distance of two peaks is about 0.25 mm and this value agrees well with the distance between two adjacent striations of Fig. 3(b).

#### 4. Conclusion

We have observed emission images using the

ICCD camera under various discharge conditions. Although our electrode substrates are specially designed for the LTS measurements, we could confirm that the basic structures of our PDP-like discharges are similar to those of real PDP discharges. Also, we could grasp the fundamental data of discharge evolutions, which will be later used for the plan of detailed measurements using the LTS method.

In this report, LTS measurements were performed under a few discharge conditions. Especially, precise measurements of the striation structure for the discharge produced in Ne/Ar (10 %) at a pressure of 100 Torr indicated that the emission profile measured using the ICCD camera was correlated with the electron temperature profile measured using the LTS method.

#### References

- 1) A. Sobel, IEEE Trans. Plasma Sci., **19** (1991) 1032.
- 2) J. P. Boeuf, J. Phys. D: Appl. Phys. **36** (2003) R53.
- 3) Y. Noguchi, A. Matsuoka, K. Uchino, and K. Muraoka, J. Appl. Phys., **91** (2002) 613.
- 4) S. Hassaballa, M. Yakushiji, Y. K. Kim, K. Tomita, K. Uchino and K. Muraoka: IEEE Trans. Plasma Science, **32** (2004) 127.
- 5) S. Hassaballa, M. Yakushiji, Y. Kim, K. Tomita, K. Uchino, and K. Muraoka, Proceedings of the tenth International Display workshop IDW'03, Fukuoka-Japan (2003) 833.
- 6) L. F. Weber, "Status and Trends of Plasma Display Device Research", 1999 International Display Research Conference (EuroDisplay '99), Berlin Germany (1999).
- 7) J. Meunier, Ph. Belenguer, J. P. Boeuf, J. Appl. Phys., **78** (1995), 731.
- 8) Th. Callegari, R. Ganter and, J. P. Boeuf, J. Appl. Phys., **88** (2000), 3905.
- 9) S. Hassaballa, K. Tomita, Y. K. Kim, K. Uchino, H. Hatanaka, Y. M. Kim, C. H. Park, and K. Muraoka, Jap. J. Appl. Phys. (submitted).
- 10) M. A. Lieberman and A. J. Lichtenberg, *Principles of Plasma Discharges and Material Processing* (New York: Wiley), (1994).